Xanthate interaction and flotation separation of H₂O₂-treated chalcopyrite and pyrite

Sultan Ahmed KHOSO[1,2], Yue-hua HU[1,2], Fei LÜ[1,2], Ya GAO[1,2], Run-qing LIU[1,2], Wei SUN[1,2]

1. School of Minerals Processing and Bioengineering, Central South University, Changsha 410083, China;
2. Key Laboratory of Hunan Province for Clean and Efficient Utilization of Strategic Calcium Containing Minerals Resources, Central South University, Changsha 410083, China

Abstract: This study investigated the effects of H_2O_2 treatment on xanthate interaction and flotation separation of chalcopyrite and pyrite by making use of a series of laboratory flotation experiments and surface analysis techniques. Flotation test results showed that H_2O_2 treatment influenced the flotation behaviors of the two minerals; however, flotation of pyrite was depressed more significantly than that of the chalcopyrite. Under well-controlled H_2O_2 concentration, the selective separation of chalcopyrite from pyrite was realized at pH 9.0, at which the recovery of chalcopyrite was over 84% and that of pyrite was less than 24%. Zeta potential, UV−visible and IR spectrum measurements revealed that the collector interacted differently with the two minerals after H_2O_2 treatment, and the surface of chalcopyrite adsorbed much greater amount of xanthate than that of the pyrite. IR and XPS analyses showed that the H_2O_2 treatment significantly changed the surface properties of pyrite to very hydrophilic species that inhibited the adsorption of collector and thus depressed the floatability of pyrite. While, the surface of chalcopyrite remained mildly inert to H_2O_2, as a result, the adsorption of xanthate and its oxidation to dixanthogen were very effective, which enhanced the flotation of chalcopyrite.

Key words: H_2O_2 treatment; selective separation; xanthate interaction; chalcopyrite; pyrite

1 Introduction

Pyrite (iron disulfide, FeS_2) is the dominant gangue mineral in flotation separation of multiple sulfide minerals [1]. Copper-containing sulfide minerals often coexist with the pyrite in the natural ore deposits. Pyrite is readily floatable mineral until pH 11 in the presence of thiol collectors, such as xanthate [2]. Consequently, the misreporting of pyrite in the flotation concentrates dilutes the grade of concentrates by increasing the contents of sulfur and iron, and causes the environmental pollution through SO_2 emissions during smelting processes [3−5]. Hence, there are several economic and environmental benefits of pyrite rejection from natural ores before their pyroprocessing.

Routinely, the lime and cyanides are generally used in the copper ore industry as the main depressants of pyrite floatability. However, the obvious drawbacks of using these inorganic reagents are that they are very expensive and hazardous to human and environment. To replace highly toxic depressants with environmentally benign reagents, several organic polymers have also been used. The organic depressants have their own benefits of the environmental friendliness, superior selectivity, widely available and cost-effective characteristics [2]. The most common organic depressants include dextrin [6], biopolymer [7], tannin [8], chitosan [2] and lignosulphonates [3]. The majority of these polymers exhibited promising possibilities in the pyrite rejection while they are used in the laboratory flotation experiments under carefully controlled conditions. However, the pyrite generally exhibits different floatability performances in different mineral deposits, where the lattice defect and surface structure inhomogeneity of pyrite are inconsistent [9,10]. All these characteristics create difficulties for finding an effective depressant of pyrite for copper ore industry.

Extensive literature indicates that the complexity or ease of the selective flotation separation of sulfide minerals is always dominated by the level of surface oxidation. The surfaces of the sulfide minerals are very sensitive to the oxidation procedures and the extent of surface oxidation is largely dependent on the mineral type; pyrite and galena are comparatively more sensitive to oxidation, followed by the sphalerite and chalcopyrite [11]. For those reasons, the selective separation of sulfide minerals by means of the oxidative treatment procedures is gaining importance day by day. Various oxidizing agents such as sodium hypochlorite (NaClO), manganese dioxide (MnO_2), oxygen (O_2), hydrogen peroxide (H_2O_2) and ozone (O_3) have been employed in the flotation technology for the selective separation of sulfides minerals [12,13].

Among others, the H_2O_2 treatment is relatively simple, cost-effective and less hazardous to human and environment. Using H_2O_2 treatment, the successful separation of the molybdenite and chalcopyrite minerals was conducted by HIRAJIMA et al [12,13]. The improved recovery of copper metal from the nickel-bearing minerals in the real ore processing was achieved at very low concentrations of H_2O_2 [14]. Literatures pertaining to the comminution of sulfide minerals indicate that the H_2O_2 formed during the milling of minerals had significant effects on their flotabilities [15,16]. Moreover, the extents of the surface oxidation of pyrite by H_2O_2 are much greater than those of the other sulfide minerals [15], which may be due to the higher affinity of hydroxyl and hydroperoxyl radicals of H_2O_2 towards the Fe(II) and Fe(III) metal ions on pyrite surface (Fenton reaction).

Therefore, by considering its different reactivity behaviors with different minerals of the complex mineralogical structures, we also hypothesized that H_2O_2 could be a potential depressant of pyrite in Cu−Fe flotation circuits with xanthate as the collector. In this regard, this study investigated the effects of H_2O_2 treatment on the xanthate interaction and floatability of chalcopyrite and pyrite and their selective separation using an industrial grade sodium butyl xanthate (SBX) as the collector. The flotation behavior and mechanism were investigated through a series of single and binary mineral selective flotation experiments, supplemented by the zeta potential measurements, UV−visible spectrum analysis, infrared (IR) spectrum analysis and X-ray photoelectron spectroscopy (XPS).

2 Experimental

2.1 Minerals and reagents

Pure samples of pyrite and chalcopyrite minerals were received from Yunfu, Guangdong Province, China.

The XRD and XRF analyses, shown in Fig. 1 and Table 1, respectively, confirmed the purity of pyrite and chalcopyrite samples. The samples were carefully handpicked, crushed and ground in the laboratory porcelain mill and sieved to obtain the maximum amount of 38−74 μm fraction for flotation experiments. The materials with undersize <38 μm were further ground to ≤5 μm fraction for the X-ray diffraction (XRD) and X-ray fluorescence (XRF) analyses, zeta potential measurements, UV−visible spectrum, IR spectrum and XPS spectrum measurements. The ground samples were stored in the sealed glass bottles under the well-controlled conditions to protect them from oxidation. However, before using any measurement, the ground samples were mixed with 50 mL HNO_3 solution with a concentration of 1 mol/L and treated under the ultrasonication for 1 min according to Ref. [13]. The resulting suspension was filtered, rinsed with ultrapure water, subsequently immersed in acetone under the
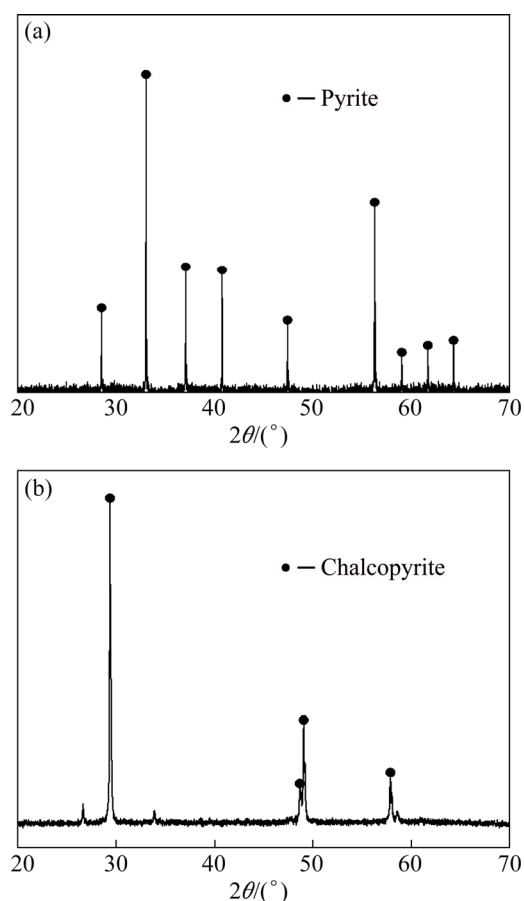
Fig. 1 XRD patterns of pure mineral samples of pyrite (a) and chalcopyrite (b)

Table 1 XRF results of pure mineral samples (wt. %)

Mineral	Cu	Fe	S	Si	Ca	Mg
Chalcopyrite	30.43	27.58	30.46	0.97	0.66	0.71
Pyrite	−	43.83	49.59	1.11	0.56	0.53

vacuum, and finally freeze-dried over 24 h. The purpose of this step was the removal of the external surface oxidation products from the mineral surfaces.

Sodium butyl xanthate (SBX, industrial grade with the purity greater than 85%) from the Chemical Factory of Zhuzhou, China, was used as the collector in flotation experiments. The analytical grade H_2O_2 (30%, mass fraction) was used for the surface oxidation treatments. The analytical grade terpineol (purity greater than 95%) from Guangdong Xilong Chemical Co., Ltd., was used as the frothing agent. The analytical grade sodium hydroxide (NaOH) and hydrochloric acid (HCl) were used to maintain the pH of the solutions. The deionized (DI) water with a resistivity of 18.2 MΩ·cm was used in all experiments.

2.2 Mineral treatment with H_2O_2

The ground powder of the representative sample of chalcopyrite or pyrite (2 g) was mixed with 30 mL DI water in a 50 mL-beaker, and the pH of the suspension was adjusted to the required level by adding HCl or NaOH under the continuous stirring at 650 r/min. Afterwards, the required concentration of H_2O_2 (1−11 mmol/L) was added into the suspension and conditioned for the total time of 3 min. The H_2O_2 addition can affect the pulp pH; therefore, the pH of the pulp was regularly maintained at the required value. Finally, the treated suspension was used in the subsequent flotation tests, or filtered and freeze-dried for the further surface analysis measurements mentioned above.

2.3 Flotation experiments

Single and binary mineral selective flotation experiments were performed in the XFG flotation machine (Exploring Machinery Plant, Changchun, China) with a 40 mL-plexiglass cell at an impeller speed of l650 r/min. In each of the single mineral tests, 2 g of the untreated mineral or H_2O_2-treated mineral suspension from Section 2.2 was transferred to a 40 mL-plexiglass cell. Following the pH adjustment with a stirring time of 2 min, the collector SBX was added to the suspension and conditioned for 3 min. Afterwards, the terpineol (1 μL) was added to the cell with a conditioning time of 1 min, and the froth and sink products were collected for 5 min. Both sink and froth fractions were oven-dried at 60 °C for 12 h and then weighed for the recovery calculation. The experiments were repeated three times and the average recovery was reported as the final value. The standard deviation, represented by an error bar, was determined using the mean of the three measurements under the same experimental conditions.

In each of the binary mineral selective flotation tests, the H_2O_2-treated minerals were manually blended in a 1:1 mass ratio for use as the flotation feed with the chemical composition listed in Table 2. The flotation procedure and the dosage and the addition order of the collector and frother used in the binary mineral selective flotation systems were the same as that of single mineral flotation except for the flotation feed. However, the recovery and grade of minerals in the binary mineral selective flotation systems were determined from the solid mass distribution between the concentrate and tailings and their chemical assays.

Table 2 XRF results of mixture of chalcopyrite and pyrite treated by H_2O_2 (wt.%)

Cu	Fe	S	Si	Ca	Mg	Others
15.55	34.38	43.58	1.01	0.43	0.57	Bal.

2.4 Zeta potential measurements

Zeta potential measurements were conducted using a ZETASIZER Nano-Zs90 series (Malvern Instruments, UK). All of the measurements were performed at room temperature ((25±1) °C) with 1 mmol/L KNO_3 as the background electrolyte solution. The mineral suspension was prepared by dispersing 0.02 g of the treated or untreated minerals into a 50 mL-beaker containing 40 mL of the KNO_3 solution, and then magnetically stirred for 10 min in the presence and absence of SBX. After permitting the coarser grains to settle for 5 min, the pH of the suspension was noted and the supernatant containing the finer particles was transferred to a capillary cell for measurements. The zeta potential measurements were determined three times for each sample, and the average was reported as the final value. The standard deviation was also calculated as described previously.

2.5 UV–visible spectrum analysis

The UV−visible spectra of the SBX solutions before and after the interaction with minerals were recorded using a 201 UV−visible spectrophotometer (Shimazu, Japan). In each of the measurements, the mineral suspension was prepared by dispersing 2 g of the treated or untreated minerals into a 40 mL-beaker containing 35 mL of the DI water, and then magnetically stirred for 10 min in the presence of collector SBX with a pre-determined concentration. Following the centri-fugation process of the resulting solution at 9000 r/min for 20 min, the absorbance of the supernatant was determined using the quartz colorimetric utensil. All of the measurements were performed at room temperature ((25±1) °C).

2.6 Infrared spectrum analysis

The infrared (IR) spectra of the mineral samples before and after the treatment with H_2O_2 and SBX were

recorded in the wavenumber range from 4000 to 400 cm^{-1} using the IR Affinity−1 spectrometer (Shimadzu Corporation, Kyoto, Japan). For this acquiring IR spectra of the minerals, 1.0 wt.% of the required mineral sample was mixed with the spectroscopic grade KBr. Mineral samples were prepared as follows: 1.0 g of the ground pyrite or chalcopyrite mineral before and after the treatment with H_2O_2 was dispersed into a 40 mL-plexiglass cell containing 35 mL DI water and conditioned for 15 min with and without the pre-determined dosage of SBX. Finally, the resulting suspensions were filtered, washed three times with DI water, and freeze-dried for 24 h prior to IR analysis. All of the measurements were performed at room temperature ((25±1) °C).

2.7 X-ray photoelectron spectroscopy analysis

The X-ray photoelectron spectra (XPS) of Fe 2p, Cu 2p, S 2p and O 1s were recorded from the surface of pyrite and chalcopyrite using a 1063 XPS spectrometer (Thermo Fisher Scientific, USA) with Al K$_\alpha$ as the sputtering source at 12 kV and 6 mA. The total spectral energy and the step size were set to be 100.0 and 1.0 eV, respectively. The sample preparation procedure was the same as that described in Section 2.6. All the measurements were performed at room temperature ((25±1) °C). The collected data were analyzed using the software XPS Peak (Version 4.1).

3 Results and discussion

3.1 Single mineral flotation

Figure 2 shows the flotation behaviors of pyrite and chalcopyrite before and after the treatment with H_2O_2 as a function of pH in the presence of SBX. Before the H_2O_2 treatment, both the pyrite and chalcopyrite followed the same flotation trends with SBX and their recoveries were more than 80%, until pH 10. This result indicated that SBX was significantly adsorbed on the surfaces of both minerals and thus enhanced their flotabilities in the wide range of pH 5−10. After the treatment with H_2O_2, the flotabilities of pyrite and chalcopyrite were dropped simultaneously and the pH had a profound effect on their recoveries. Interestingly, the depression of H_2O_2-treated pyrite was much greater than that of H_2O_2-treated chalcopyrite in the studied pH range of 5−11, indicating that H_2O_2 treatment had a much greater affinity towards the pyrite surface which inhibited the adsorption of collector. As seen in Fig. 2, the recovery of pyrite was steeply dropped from 83% to 33% at pH 5 and then decreased further to become very low (20%) by increasing the pH from 5 to 11. The

recovery of chalcopyrite was also dropped from 81% to 68% at pH 5 and then increased with increasing pH and reached about 80% at pH 11. This implied that the H_2O_2 treatment had very limited influence on the chalcopyrite, as a result, its surface adsorbed greater amount of the collector that enhanced its flotation.
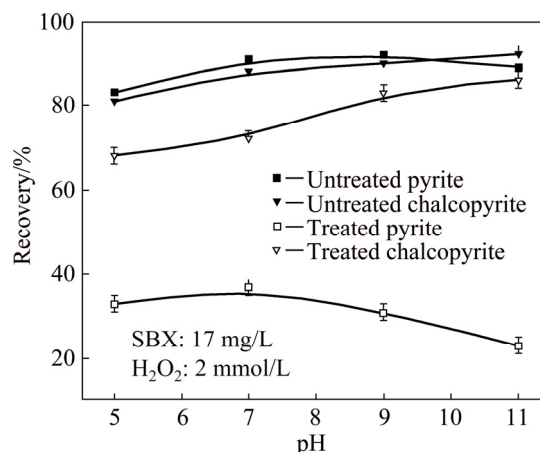

Fig. 2 Flotation behaviors of chalcopyrite and pyrite before and after treatment with H_2O_2 in the presence of SBX

The results shown in Fig. 2 indicated that the optimum depression of pyrite and the maximum recovery difference between the chalcopyrite and pyrite after the treatment with H_2O_2 were achieved at pH 9 or above. Therefore, single mineral floatability tests were further extended by fixing the pH around 9 and varying the concentrations of H_2O_2. Figure 3 displays that the floatation recoveries of pyrite and chalcopyrite were dropped simultaneously with increasing the H_2O_2 concentration. However, a remarkable difference was again noted between the flotation recoveries of the two minerals at the low H_2O_2 concentration. As seen, the recovery of pyrite was dropped significantly from 40% to 12% in the H_2O_2 concentration range of 1−7 mmol/L, and then became stable and unchanged with further

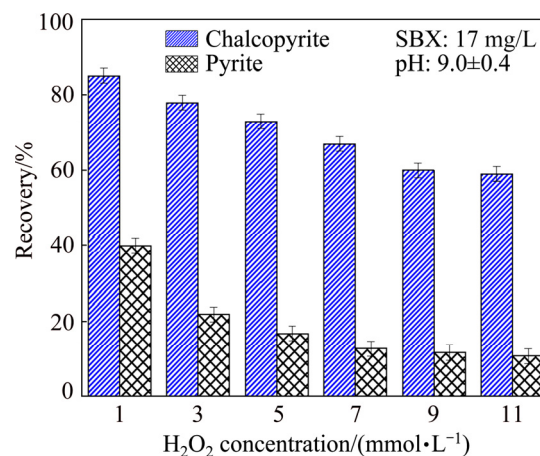**Fig. 3** Flotation recoveries of chalcopyrite and pyrite as function of H_2O_2 concentration in the presence of SBX

increasing of the H_2O_2 concentration. While, in the same H_2O_2 concentration range, the recovery of chalcopyrite was slightly decreased from 85% to 70%, and the excessive concentration greater than 7 mmol/L had a slightly negative impact on the chalcopyrite recovery. Single mineral floatability results therefore suggested that the separation window between the chalcopyrite and pyrite can be possible at low alkaline pH after their treatment with the low concentration of H_2O_2 in the presence of SBX as the collector.
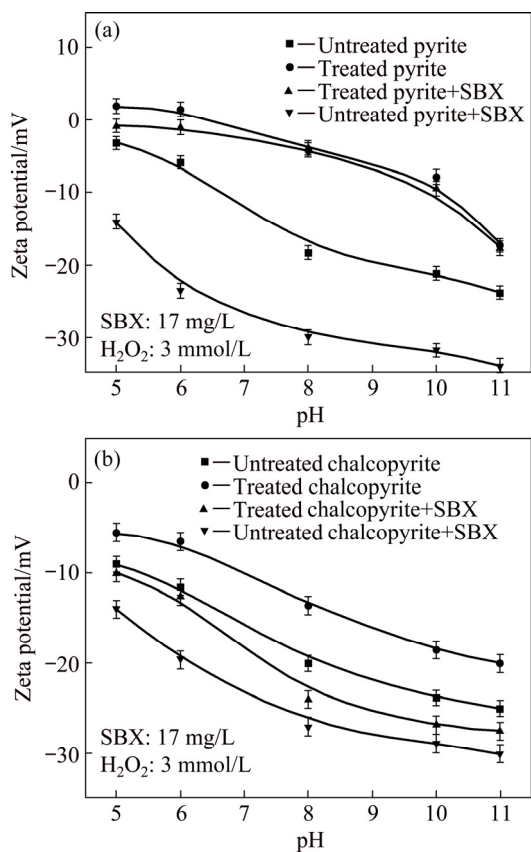
3.2 Zeta potential

The surface charge of the sulfide minerals containing copper, lead and iron varies significantly with the pre-treatment actions. In this regard, the zeta potential measurements were performed to monitor the changes in electric charge on the surfaces of pyrite and chalcopyrite before and after the treatment with H_2O_2 and SBX. Figure 4 shows that the zeta potential of untreated minerals was negative at the tested pH (5−11) and had an isoelectric point (IEP) less than pH 5; this result is consistent with the previous literatures [1,17]. Furthermore, the zeta potentials of these minerals were gradually decreased with increasing pH due to adsorption of hydroxyl ions on their surfaces. In the presence of SBX alone, the zeta potentials of both minerals were

Fig. 4 Zeta potentials of pyrite (a) and chalcopyrite (b) before and after treatment with H_2O_2 in the absence and presence of SBX

significantly decreased, indicating that xanthate anions were strongly absorbed onto the surfaces of pyrite and chalcopyrite; this result therefore validated the single mineral floatability tests in which both minerals were highly floatable with SBX.

After the treatment with H_2O_2, the zeta potentials of chalcopyrite and pyrite shifted to more positive side, showing that the H_2O_2 treatment modified their surface characteristics. However, compared with chalcopyrite, the positive shift in the zeta potential of pyrite particles was much more obvious as its IEP shifted to the higher pH of about 6.5, indicating that H_2O_2 treatment had much greater affinity on the surface of pyrite than that of the chalcopyrite. Moreover, the subsequent addition of SBX did not significantly decrease the zeta potential of H_2O_2-treated pyrite, representing that the pyrite surface was highly oxidized by H_2O_2. Therefore, the strongest depression of H_2O_2-treated pyrite in single mineral flotation tests may be attributed to no or less adsorption of the collector on the pyrite surface. On the other hand, the zeta potential of H_2O_2-treated chalcopyrite surface was greatly decreased to more negative values after the subsequent addition of SBX, indicating that the adsorption of the collector on the chalcopyrite surface was more efficient. The effective adsorption of SBX onto the chalcopyrite might be due to the lower surface oxidation by H_2O_2 treatment, as indicated by the minor shifts in the zeta potential of chalcopyrite surface after the H_2O_2 treatment. Therefore, the higher flotabilities of H_2O_2-treated chalcopyrite in single mineral flotation tests may be attributed to the effective adsorption of collector onto chalcopyrite surface.

The oxidative treatment can dissolve the mineral surfaces into their respective metal species in the solution and the precipitation of these species onto the surfaces results in the increase of surface potentials of minerals [18]. The FeO, FeOOH and $Fe_2(SO_4)_3$ from the pyrite surface and $Cu(OH)_2$, Cu_2O and CuO from the chalcopyrite surface are noted as the most dominant oxidation species and their formation and concentration are largely dependent on the degree of oxidation [18]. Moreover, the FeO, FeOOH and $Fe_2(SO_4)_3$ are relatively strong hydrophilic species that greatly inhibit the adsorption of collector and its oxidation to dixanthogen on the mineral surfaces and thus depress their flotabilities [18]. Several other investigations have confirmed that the xanthate has much higher interaction with the copper hydroxide precipitates compared with iron hydroxides or sulfate species [19]. Therefore, the lower adsorption of collector on the pyrite surface may be attributed to the presence of FeO, FeOOH and $Fe_2(SO_4)_3$ species resulted from the H_2O_2 treatment. To the contrary, the effective adsorption of collector on the

chalcopyrite surface may be attributed to the presence of lower surface oxidation products by H_2O_2.

3.3 UV−visible spectrum

Zeta potential results have shown that the H_2O_2 treatment affects the adsorption of collector onto the mineral surfaces. To validate the zeta potential measurements, UV−visible spectra were recorded to know the interaction of SBX with mineral surfaces. As can be seen in Fig. 5, before the interaction with minerals there was an intensive xanthate peak around 301 nm [20], which then significantly decreased or disappeared from the solution when xanthate interacted with pyrite and chalcopyrite before their treatment with H_2O_2. Apparently, the intensity of xanthate peak was also decreased after the interaction with H_2O_2-treated chalcopyrite, thus confirming the zeta potential results that the xanthate was strongly adsorbed onto H_2O_2-treated chalcopyrite surface. The significant depletion of xanthate peak after the interaction with untreated minerals and the H_2O_2-treated chalcopyrite indicated the complete adsorption of xanthate on their surfaces. The xanthate was chemically adsorbed on the surfaces of pyrite and chalcopyrite and formed the chemical coordination with iron (Fe) and copper (Cu) metals on their surfaces through its sulfur (S) atoms. Therefore, a broad absorbance appeared at 420−450 nm in the spectra of untreated minerals and H_2O_2-treated chalcopyrite might be attributed to Fe—S and Cu—S bonds [20]. To the contrary, the intensity of the xanthate peak was not significantly decreased after the interaction with H_2O_2-treated pyrite, indicating that less amount of collector was adsorbed on the H_2O_2-treated pyrite. These results are in good agreement with zeta potential measurements and showed that there was the weak interaction between the xanthate and H_2O_2-treated pyrite surface.
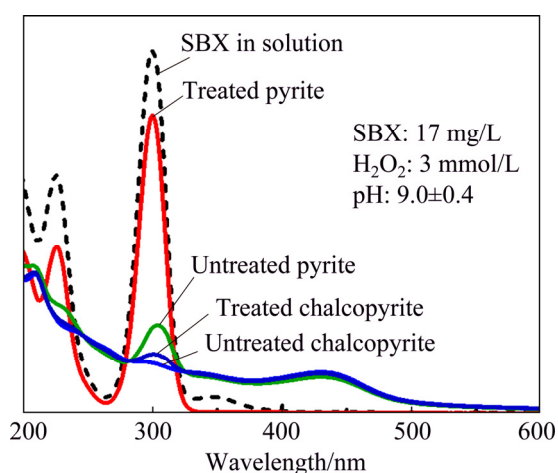
Fig. 5 UV−visible spectra of SBX solution before and after interaction with minerals

3.4 Infrared spectrum

Infrared (IR) spectrum spectroscopy is one of the best tools to obtain the detail understanding of the surface properties of minerals and adsorption mechanism of flotation reagents on mineral surfaces. The IR spectra of the treated and untreated minerals in the absence and presence of SBX are shown in Fig. 6. In the IR spectra of SBX-treated minerals, all the possible peaks of xanthate adsorptions were observed on the chalcopyrite and pyrite surfaces around 1145, 1275 and 2926 cm^{-1} corresponding to the stretching vibrations of the xanthate−iron/copper compounds, dixanthogen and CH_2 groups, respectively [9], indicating that SBX was strongly absorbed on the pyrite and chalcopyrite surfaces before the treatment with H_2O_2. This validated the zeta potential measurements and UV−visible spectrum analysis that xanthate was substantially adsorbed on the untreated minerals and thus enhanced their floatability.
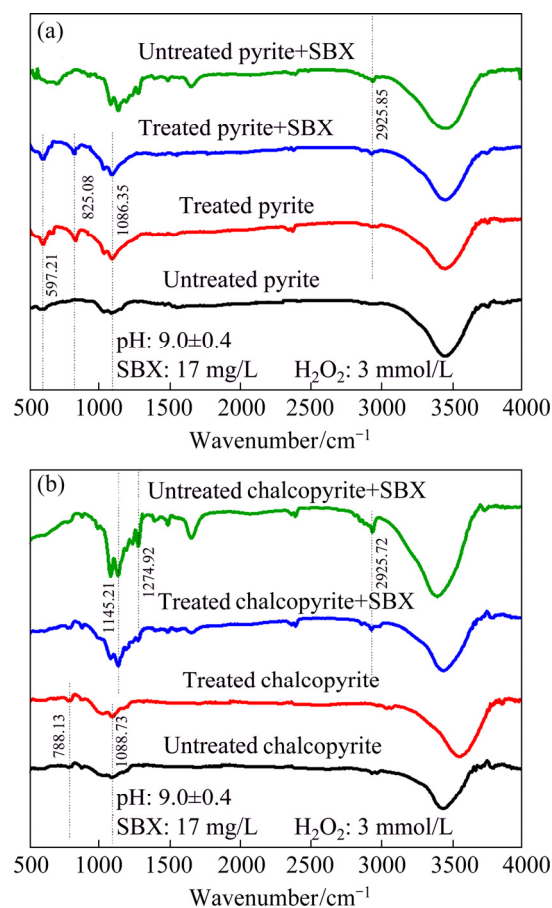
Fig. 6 Infrared spectra of pyrite (a) and chalcopyrite (b) before and after treatment with H_2O_2 in the absence and presence of SBX

The IR spectra of chalcopyrite and pyrite after the treatment with H_2O_2 revealed a significant difference that was actually contributed to their different interaction behaviors with SBX and thus different flotation trends. In the spectra of H_2O_2-treated pyrite, the characteristic

peaks around 1086.35 and 597.21 cm^{-1} were assigned to SO_4^{2-} and that at 825.08 cm^{-1} corresponded to the stretching vibrations of FeO and FeOOH [21], indicating that the pyrite surface was highly oxidized after the treatment with H_2O_2. Hence, no or less adsorption peaks of xanthate on the H_2O_2-treated pyrite surface revealed that the adsorption of collector and its oxidation to dixanthogen were significantly blocked by the hydrophilic species on pyrite surface [18,22]. Compared with pyrite, there was very limited effect of H_2O_2 treatment on the chalcopyrite surface; minor peaks of SO_4^{2-} and $Cu(OH)_2$ were noted in the spectra of H_2O_2-treated chalcopyrite. However, the treated and untreated chalcopyrite contained some weaker signals of SO_4^{2-} (1088.73 cm^{-1}) and CuO or CuO_2 (788.13 cm^{-1}) [23]. Thus, the slight depression of chalcopyrite in the single mineral flotation tests may be due to the presence of these oxidized species on its surface [24]. In addition, the strong adsorption peaks of SBX and its oxidation to dixanthogen on the H_2O_2-treated chalcopyrite surface can be seen around 1145.21 cm^{-1} (copper–xanthate), 1274.92 cm^{-1} (dixanthogen) and 2925.72 cm^{-1} (CH_2), indicating that the H_2O_2-treated chalcopyrite still adsorbed much greater amount of SBX. Apparently, the extent of surface oxidation of pyrite was much greater than that of chalcopyrite, which might be due to the strong affiliation of hydroxyl and hydroperoxyl radicals of H_2O_2 with ferrous/ferric iron ions of the pyrite through the Fenton reaction mechanism [25]. The difference in the mineralogical structure of the pyrite and chalcopyrite may also be one reason of their different interaction behaviors with H_2O_2 [11,24].

The IR spectrum results therefore confirmed the zeta potential measurements and UV−visible spectrum analysis and showed that the adsorption of collector and its oxidation to dixanthogen on the H_2O_2-treated pyrite surface were significantly inhibited by the presence of FeO, FeOOH and SO_4^{2-} hydrophilic species resulted from the H_2O_2 treatment of pyrite. To the contrary, due to very limited effects of H_2O_2 treatment on the chalcopyrite surface, the adsorption of collector and its oxidation to dixanthogen on the H_2O_2-treated chalcopyrite surface were more effective.

3.5 XPS spectrum

The IR spectrum results have shown that different extents of the surface oxidation species on pyrite and chalcopyrite contributed to their different interaction behaviors with SBX. It is also widely believed that hydrophilic or hydrophobic characteristics of the sulfide minerals are greatly affected by the chemical state of their important surface species such as Fe, Cu, S and O [13]. Therefore, in this work, the high resolution spectra of Fe 2p, Cu 2p, S 2p and O 1s species were also

recorded from the surfaces of pyrite and chalcopyrite in order to gain a full understanding of the surface chemistry of these minerals before and after the treatment with H_2O_2.

In the high resolution XPS spectra of untreated pyrite shown in Fig. 7, the characteristic peaks at 707.91 and 720.71 eV from the Fe 2p spectra and 161.74 and 162.82 eV from the S 2p spectra corresponded to spin-orbitals of $2p_{3/2}$ and $2p_{1/2}$, respectively [14,22]. The O 1s spectra indicated that the peaks around 529.90 and 530.42 eV corresponded to O^{2-} and —OH,
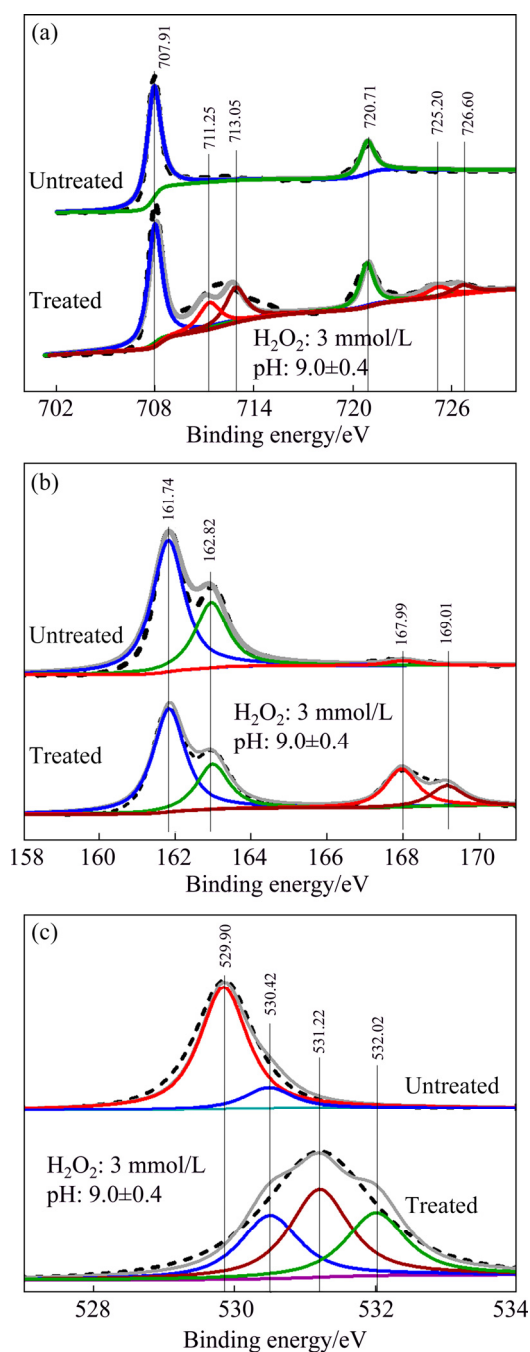
Fig. 7 High resolution XPS spectra of pyrite before and after treatment with H_2O_2: (a) Fe 2p; (b) S 2p; (c) O 1s

respectively [26]. It is generally considered that the Fe(III) and Fe(II) oxides have the binding energies around 530.20 eV [27], thus the peak at a binding energy of 530.42 eV can be allotted to iron oxide. As shown, after the treatment with H_2O_2, all of the three spectra indicated much greater changes to the surface of pyrite, indicating that the pyrite surface was sufficiently oxidized by H_2O_2. In the Fe 2p spectra of treated pyrite, the peaks at 711.25 and 725.20 eV and 713.05 and 726.60 eV were assigned to the binding energies of FeO/FeOOH and $Fe_2(SO_4)_3$ species, respectively [22,28]. The S 2p spectra treated by H_2O_2 confirmed the presence of $Fe_2(SO_4)_3$ peaks at 167.99 and 169.01 eV [14,29]. The deconvolution of the O 1s spectra also supports the FeO/FeOOH and $Fe_2(SO_4)_3$ peaks at 531.22 and 532.02 eV, respectively [27,29]. These results therefore confirmed the IR spectrum measurements and indicated that the surface of pyrite was significantly oxidized by H_2O_2 treatment and its surface contained sufficient amount of FeO/FeOOH and $Fe_2(SO_4)_3$ like hydrophilic species.

In the high resolution XPS spectra of chalcopyrite shown in Fig. 8, the binding energies at 932.12 and 951.90 eV from Cu 2p spectra, 708.14 and 721.61 eV from Fe 2p spectra, and 161.44 and 162.58 eV from S 2p spectra corresponded to spin-orbitals of $2p_{3/2}$

and $2p_{1/2}$ respectively [13,14,30]. In the O 1s spectra, the binding energies around 529.80 and 530.43 eV corresponded to the lattice oxygen and adsorbed oxygen, respectively [31]. Some weaker binding energies around 933.17 and 935.07 eV from the Cu 2p spectra and 530.43 eV from O 1s spectra signified the presence of CuO or CuO_2 peaks on the untreated chalcopyrite surface [12,27,31−34], indicating that chalcopyrite surface was also slightly oxidized during the sample preparation. By comparing the spectra of chalcopyrite before and after the treatment with H_2O_2, no significant changes were noted, thus suggesting that there were the negligible effects of H_2O_2 on the chalcopyrite surface. As seen clearly, there were no significant evidences of the SO_4^{2-} species from the S 2p and O 1s spectra of H_2O_2-treated chalcopyrite. Hence, these results were also consistent with the IR spectrum analysis and revealed that the chalcopyrite surface remained mildly inert to H_2O_2 treatment at the investigated concentrations.

3.6 Selective flotation

After gaining a full understanding on the effects of H_2O_2 treatment on the xanthate interaction and floatability of individual minerals, further selective flotation experiments on the mixture of H_2O_2-treated minerals were carried out at pH 9 with SBX
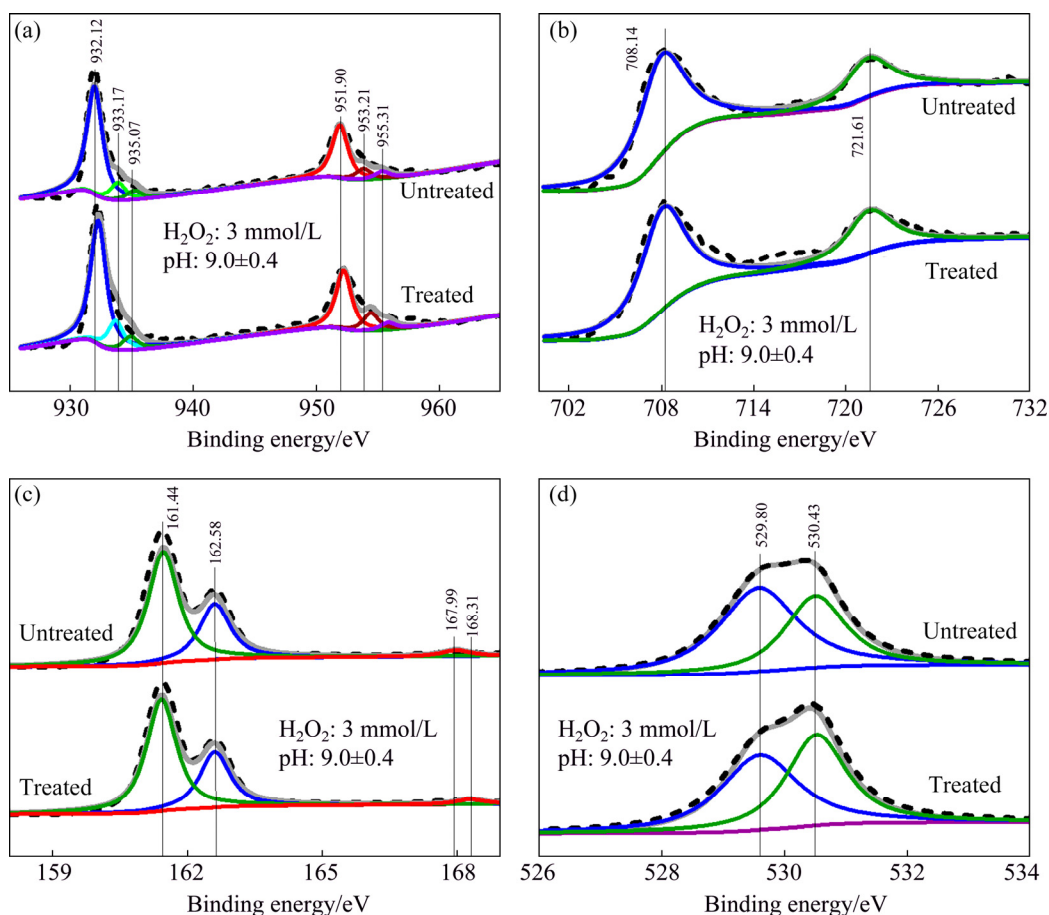
**Fig. 8** High resolution XPS spectra of chalcopyrite before and after treatment with H_2O_2: (a) Cu 2p; (b) Fe 2p; (c) S 2p; (d) O 1s

concentration of 17 mg/L. For this, the minerals were manually mixed in a mass ratio of 1:1 for use as the flotation feed with the chemical compositions listed in Table 2. In addition to the grades and recoveries of chalcopyrite and pyrite, the mineral recovery differences (i.e., $R_{chalcopyrite} - R_{pyrite}$) and the separation selectivity index (i.e., recovery ratio of chalcopyrite to pyrite) were also calculated and presented in Fig. 9.

In Fig. 9(a), the sufficient improvement in the grade and recovery of chalcopyrite indicated that the selective separation between the chalcopyrite and pyrite occurred by increasing H_2O_2 concentration from 1 to 5 mmol/L. To attain a balance between the recovery and grade, so called "trade-off domain", was found in H_2O_2 concentration range of 3−5 mmol/L. Within this concentration range, both the grade and recovery of the chalcopyrite reached 84.71% and 83.11%, respectively, and those of pyrite were less than 20%. However, the excessive concentration of H_2O_2 had a slightly negative impact on the chalcopyrite recovery. Figure 9(a) further showed that the flotation concentrate contained a chalcopyrite grade improvement of nearly 70% compared to that of the initial flotation feed in Table 2.

A similar trend can be seen in Fig. 9(b), both the recovery difference and separation selectivity index of
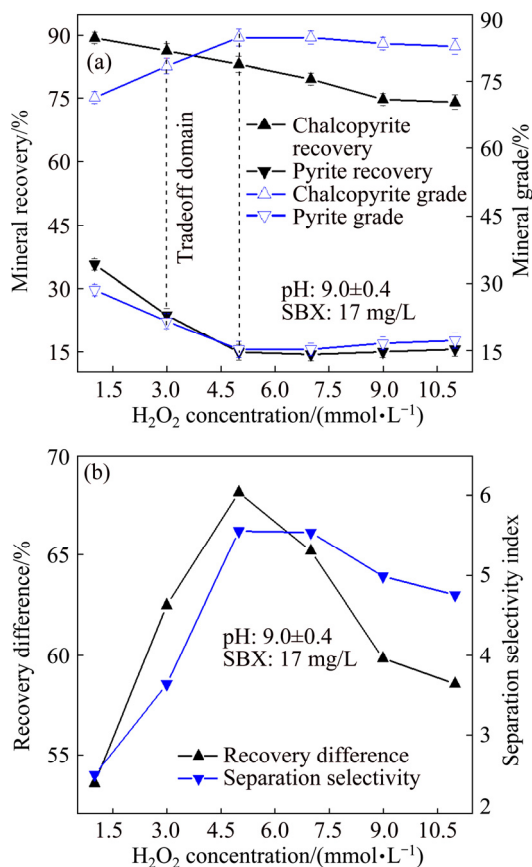
two minerals were increased in the straightforward manner by increasing H_2O_2 concentration up to 5 mmol/L. At 5 mmol/L H_2O_2, both the recovery difference and the selectivity index of these minerals reached at the maximum values about 68.14% and 5.58%, respectively. Figure 9(b) also showed that the excessive dosage of H_2O_2 had somewhat negative influences on the selective separation of chalcopyrite and pyrite, indicating that the same phenomenon occurred in the binary mineral selective flotation as that in the single mineral floatability tests. The selective flotation results shown in Fig. 9 clearly indicated that the surface of H_2O_2-treated chalcopyrite adsorbed much greater amount of SBX than that of H_2O_2-treated pyrite. Moreover, when the H_2O_2-treated minerals were placed together in the suspension, the SBX was preferentially adsorbed onto the chalcopyrite surface and thus allowed it to float in the mixture.

From all of the microflotation results, it was noted that the excessive concentration of H_2O_2 has a negative impact on the chalcopyrite recovery; and thus, on the selective separation of chalcopyrite and pyrite. NOOSHABADI et al [15] also reported that H_2O_2 formed during the milling of sulfide minerals has the significant effects on their floatabilities. Both pyrite and chalcopyrite in the presence of H_2O_2 induce the oxidation of their surfaces with the formation of the hydrophilic FeOOH and SO_4^{2-} species that cause their depression in flotation. HIRAJIMA et al [12,13] conducted the selective flotation of molybdenite from chalcopyrite with H_2O_2 and their results suggested that the higher concentration of H_2O_2 resulted in the lower floatability of chalcopyrite. CHIMONYO et al [14] worked on the real ore containing copper and nickel minerals and reported that at very low concentrations of H_2O_2, the recovery of copper increased significantly.

Based on the above reported studies, we also hypothesized that at the high concentration of H_2O_2, the sulfate species may be formed on the chalcopyrite surface, which resulted in poor adsorption with xanthate. However, under the well-controlled conditions, the H_2O_2 treatment can produce the effective separation between chalcopyrite and pyrite at slight alkaline pH in the presence of SBX, as well demonstrated in Fig. 9. Therefore, the H_2O_2, which is relatively non-hazardous, widely available and cost-effective, has a great potential to be used as an alternative depressant in the Cu−Fe conventional flotation circuits with xanthate as the collector.

Fig. 9 Selective flotation results: (a) Recovery and grade of minerals; (b) Separation selectivity index and recovery differences of minerals

4 Conclusions

(1) The H_2O_2 treatment depressed the flotation of pyrite much stronger than that of the chalcopyrite with

sodium butyl xanthate (SBX) as the collector. The best selective separation between the chalcopyrite and pyrite was realized at pH 9, at which the recovery of chalcopyrite was nearly to 84% and that of pyrite was less than 20%.

(2) The zeta potential, UV−visible and IR spectrum measurements indicated that the interaction and adsorption of xanthate on the surfaces of H_2O_2-treated chalcopyrite were much greater than that on H_2O_2-treated pyrite.

(3) The IR and XPS spectrum measurements further indicated that the surface of pyrite was seriously oxidized and covered with the hydrophilic FeO, FeOOH and $Fe_2(SO_4)_3$ species after the treatment with H_2O_2. While, the surface of chalcopyrite remained mildly inert to H_2O_2 at the investigated concentrations.

(4) Different extents of oxidation species on pyrite and chalcopyrite surfaces after the treatment with H_2O_2 contributed to their different interaction behavior with xanthate and thus the different flotation trends.

References

[1] KHOSO S A, HU Yue-hua, LIU Run-qing, TIAN Meng-jie, SUN Wei, GAO Ya, HAN Hai-sheng, GAO Zhi-yong. Selective depression of pyrite with a novel functionally modified biopolymer in a Cu−Fe flotation system [J]. Minerals Engineering, 2019, 135: 55−63.

[2] HUANG Peng, CAO Ming-li, LIU Qi. Selective depression of pyrite with chitosan in Pb−Fe sulfide flotation [J]. Minerals Engineering, 2013, 47(3): 45−51.

[3] MU Yu-fan, PENG Yong-jun, LAUTEN R A. The mechanism of pyrite depression at acidic pH by lignosulfonate-based biopolymers with different molecular compositions [J]. Minerals Engineering, 2016, 92: 37−46.

[4] KHOSO S A, ABRO M I, AGHEEM M H. Mineralogical study of Zard Koh and Kulli Koh iron ore deposits of Pakistan [J]. Mehran University Research Journal of Engineering and Technology, 2017, 36(4): 1017−1024.

[5] KHOSO S A, ABRO M I, AGHEEM M H. Evaluation of mesh of liberation of Zard Koh and Kulli Koh iron ores of Pakistan [J]. Mehran University Research Journal of Engineering and Technology, 2018, 37(4): 569−580.

[6] VALDIVIESO A L, CERVANTES T C, SONG S, CABRERA A R, LASKOWSKI J S. Dextrin as a non-toxic depressant for pyrite in flotation with xanthates as collector [J]. Minerals Engineering, 2004, 17(9): 1001−1006.

[7] MU Yu-fan, PENG Yong-jun, LAUTEN R A. The depression of copper-activated pyrite in flotation by biopolymers with different compositions [J]. Minerals Engineering, 2016, 96−97: 113−122.

[8] SARQUÍS P E, MENÉNDEZ-AGUADO J M, MAHAMUD M M, DZIOBA R. Tannins: The organic depressants alternative in selective flotation of sulfides [J]. Journal of Cleaner Production, 2014, 84(1): 723−726.

[9] WANG Zhen, QIAN Yun-lou, XU Long Hua, DAI Bo, XIAO Jun Hui, FU Kai-bin. Selective chalcopyrite flotation from pyrite with glycerine−xanthate as depressant [J]. Minerals Engineering, 2015, 74: 86−90.

[10] CHANDRA A P, GERSON A R. A review of the fundamental studies of the copper activation mechanisms for selective flotation of the sulfide minerals, sphalerite and pyrite [J]. Adv Colloid Interface Sci,

[11] HONG G, CHOI J, HAN Y, YOO K, KIM K, KIM S B, KIM H. Relationship between surface characteristics and floatability in representative sulfide minerals: Role of surface oxidation [J]. Materials Transactions, 2017, 58(7): 1069−1075.

[12] HIRAJIMA T, MIKI H, SUYANTARA G P W, MATSUOKA H, ELMAHDY A M, SASAKI K, IMAIZUMI Y, KUROIWA S. Selective flotation of chalcopyrite and molybdenite with H_2O_2 oxidation [J]. Minerals Engineering, 2017, 100: 83−92.

[13] SUYANTARA G P W, HIRAJIMA T, MIKI H, SASAKI K, YAMANE M, TAKIDA E, KUROIWA S, IMAIZUMI Y. Selective flotation of chalcopyrite and molybdenite using H_2O_2 oxidation method with the addition of ferrous sulfate [J]. Minerals Engineering, 2018, 122: 312−326.

[14] CHIMONYO W, WIESE J, CORIN K, O'CONNOR C. The use of oxidising agents for control of electrochemical potential in flotation [J]. Minerals Engineering, 2017, 109: 135−143.

[15] NOOSHABADI A J, LARSSON A, KOTA H R. Formation of hydrogen peroxide by pyrite and its influence on flotation [J]. Advanced Powder Technology, 2014, 25(3): 832−839.

[16] NOOSHABADI A J, RAO K H. Complex sulphide ore flotation: Effect of depressants addition during grinding on H_2O_2 formation and its influence on flotation [J]. International Journal of Mineral Processing, 2016, 157: 89−97.

[17] GUAN Chang-ping, YIN Zhi-gang, KHOSO S A, SUN Wei, HU Yue-hua. Performance analysis of thiocarbonohydrazide as a novel selective depressant for chalcopyrite in molybdenite−chalcopyrite separation [J]. Minerals, 2018, 8(4): 142.

[18] YIN Wan-zhong, XUE Ji-wei, LI Dong, SUN Qian-yu, YAO Jin, HUANG Shi. Flotation of heavily oxidized pyrite in the presence of fine digenite particles [J]. Minerals Engineering, 2018, 115: 142−149.

[19] SARVARAMINI A, LARACHI F, HART B. Ethyl xanthate collector interaction with precipitated iron and copper hydroxides–Experiments and DFT simulations [J]. Computational Materials Science, 2016, 120: 108−116.

[20] MIKHLIN Y, VOROBYEV S, SAIKOVA S, TOMASHEVICH Y, FETISOVA O, KOZLOVA S, ZHARKOV S. Preparation and characterization of colloidal copper xanthate nanoparticles [J]. New Journal of Chemistry, 2016, 40(4): 3059−3065.

[21] MIN Xiao-bo, LIYANG wen-jun, KE Yong, SHI Mei-qing, CHAI Li-yuan, KE Xue. Fe−FeS₂ adsorbent prepared with iron powder and pyrite by facile ball milling and its application for arsenic removal [J]. Water Science & Technology, 2017, 76(1): 192−200.

[22] XIAN Yong-jun, WANG Yi-jie, WEN Shu-ming, NIE Qi, DENG Jiu-shuai. Floatability and oxidation of pyrite with different spatial symmetry [J]. Minerals Engineering, 2015, 72: 94−100.

[23] CHIRITA P, DESCOSTES M, SCHLEGEL M L. Oxidation of FeS by oxygen-bearing acidic solutions [J]. J Colloid Interface Sci, 2008, 321(1): 84−95.

[24] PARK K, CHOI J, GOMEZ-FLORES A. Flotation behavior of arsenopyrite and pyrite, and their selective separation [J]. Materials Transactions, 2015, 56(3): 435−440.

[25] SCHOONEN M A A, HARRINGTON A D, LAFFERS R, STRONGIN D R. Role of hydrogen peroxide and hydroxyl radical in pyrite oxidation by molecular oxygen [J]. Geochimica et Cosmochimica Acta, 2010, 74(17): 4971−4987.

[26] PENG Hui-qing, WU Di, ABDELMONEM M. Flotation performances and surface properties of chalcopyrite with xanthate collector added before and after grinding [J]. Results in Physics, 2017, 7: 3567−3573.

[27] HUA Xiao-ming, ZHENG Yong-fei, XU Qian, LU Xiong-gang, CHENG Hong-wei, ZOU Xing-li, SONG Qiu-shi, NING Zhi-qiang,

FREE M L. Leaching mechanism and electrochemical oxidation on the surface of chalcopyrite in ammonia−ammonium chloride solution [J]. Journal of the Electrochemical Society, 2018, 165(10): E466−E476.

[28] ZHANG Bo, YAN Guang-hui, ZHAO Yue-min, ZHOU Chen-yang, LU Yao. Coal pyrite microwave magnetic strengthening and electromagnetic response in magnetic separation desulfurization process [J]. International Journal of Mineral Processing, 2017, 168: 136−142.

[29] YUNIATI M D, HIRAJIMA T, MIKI H, SASAKI K. Silicate covering layer on pyrite surface in the presence of silicon–catechol complex for acid mine drainage prevention [J]. Materials Transactions, 2015, 56: 1733−1741.

[30] OWUSU C, FORNASIERO D, ADDAI-MENSAH J, ZANIN M. Influence of pulp aeration on the flotation of chalcopyrite with xanthate in chalcopyrite/pyrite mixtures [J]. International Journal of Mineral Processing, 2015, 134: 50−57.

[31] PENG Hui-qing, WU Di, ABDELMONEM M. Flotation performances and surface properties of chalcopyrite with xanthate collector added before and after grinding [J]. Results in Physics, 2017, 7: 3567−3573.

[32] CHEN Jian-hua, LAN Li-hong. Depression effect of pseudo glycolythiourea acid in flotation separation of copper−molybdenum [J]. Transactions of Nonferrous Metals Society of China, 2013, 23(3): 824−831.

[33] PLESSIS R D, MILLER J D. Preliminary examination of electrochemical and spectroscopic features of trithiocarbonate collectors for sulfide mineral flotation [J]. Transactions of Nonferrous Metals Society of China, 2000, 10(1): 12−18.

[34] LIN Qing-quan, GU Guo-hua, WANG Hui, LIU You-cai, WANG Chong-qing, FU Jian-gang, ZHAO Jun-yao, HUANG Luo-luo. Recovery of molybdenum and copper from porphyry ore via iso-floatability flotation [J]. Transactions of Nonferrous Metals Society of China, 2017, 27(10): 2260−2271.

H_2O_2 处理后的黄铜矿和黄铁矿对黄药的吸附作用及其浮选分离

Sultan Ahmed KHOSO[1,2]，胡岳华[1,2]，吕 斐[1,2]，高 雅[1,2]，刘润清[1,2]，孙 伟[1,2]

1. 中南大学 资源加工与生物工程学院，长沙 410083；
2. 中南大学 战略含钙矿物资源清洁高效利用湖南省重点实验室，长沙 410083

摘 要：通过一系列浮选试验和矿物表面分析技术研究 H_2O_2 处理对黄药浮选分离黄铜矿与黄铁矿的影响。浮选试验结果表明，H_2O_2 对两种矿物的浮选行为具有一定影响，H_2O_2 对黄铁矿的抑制效果强于黄铜矿。在一定 H_2O_2 浓度条件下，黄铜矿在 pH 9.0 时可从黄铁矿中选择性分离出来，此时黄铜矿的回收率达 84% 以上，而黄铁矿回收率低于 24%。Zeta 电位、紫外−可见分光光谱以及红外光谱等分析结果表明，H_2O_2 处理后的两种矿物对捕收剂的吸附量不同，黄铜矿表面对黄药的吸附量远远大于黄铁矿表面对黄药的吸附量。红外光谱和 XPS 分析结果表明，H_2O_2 处理可大幅度提高黄铁矿表面的亲水性，从而抑制捕收剂的吸附，使其可浮性下降；而黄铜矿对 H_2O_2 不产生吸附，因此对黄药的吸附和对二黄原酸的氧化效果较好，黄铜矿的浮选回收率较高。

关键词：H_2O_2 处理；选择性分离；黄药吸附；黄铜矿；黄铁矿

(Edited by Wei-ping CHEN)